Turkish J. Eng. Env. Sci.
30 (2006) , 221 – 229.

Mass Transfer Coefficients at the Stagnation Point with Submerged Impinging Multi-Jet Flow of Fluid Electrolyte

Shaik FEROZ
M&IE Department, Caledonian College of Engineering-OMAN
e-mail: feroz@caledonian.edu.om
V. S. R. K. PRASAD
Andhra University, Department of Chemical Engineering, Visakhapatanam-INDIA
e-mail: srkpveerapaneni@hotmail.com

Received 31.08.2005

Abstract

This paper presents experimental results for the mass transfer coefficients in the impingement region of a multi-jet flow. A disc distributor containing 'N' nozzles produces multi-jets that interact in a complex manner before they reach the target surface where mass transfer occurs. In particular, the size of the distributor disc, together with its height from the target surface, and the nozzle hole diameters and arrangements are varied in the experiments to find their effects on the mass transfer coefficient. The mass transfer coefficient increases with an increase in nozzle hole and disc distributor size, and decreases with an increase in both the height of the disc distributor from the target surface and cell size. Correlations of the mass transfer coefficient with a typical flow Reynolds number are also proposed.

Key words: Multi-jets, Disc distributor, Nozzle hole, Electrolytic cell, Stagnation point.

Introduction

Jet flow is one of the techniques adopted to augment heat/mass transfer rates. It allows short flow-paths on the transfer surface, resulting in high rates of heat or mass transfer. Industrially, jet flow finds wide applications, such as in annealing of metals and plastic sheets, tempering of glass, drying of textiles, veneer, paper, and film materials, and more recently the impinging jet-cooling technique employed for electronic devices in order to meet the demand of compactness and high power consumption. This technique is also used in gas turbine operations in which the excessive thermal loading near the leading edge of the gas turbine blade inner surface can be eliminated.

The literature reveals several works on heat/mass transfer using jets in open and closed containers. Several authors (Rao et al., 1971; Martin, 1977) reported hydrodynamics with different flow regions for open and submerged jets. They suggested empirical correlations by studying the effects of various dynamic and geometric variables. Studies reported so far are based on single jets, where the transfer rates are much higher compared to multi-jets; however, high specific productivities and near uniform distribution of mass transfer coefficients over electrodes having larger dimensions can be achieved only with impinging multi-jets (Koopman and Sparrow, 1976; Nanzer et al., 1984; Chattopadhyay and Saha, 2002).

The present study aimed to investigate the effect of several parameters, including nozzle hole diameter (d_j), height of the nozzle hole assembly from the target surface (h), diameter of the nozzle hole assembly, i.e., disc distributor (D_d), and diameter of the cell (D_c) on mass transfer between submerged multi-jets issuing from the circular disc distributor onto the reacting surface normal to the jets. $J_D - Re$ format type empirical correlations are proposed for the mass transfer data obtained from the reduction of the ferricyanide ion at the stagnation point.

One may visualize the hydrodynamics of the impinging jet flow on the target surface as follows: the jets issuing from the nozzle impinge on the target surface and gradually flow radially away towards the outer edge of the target surface or the confining wall of the electrolytic cell, depending on whether it is a free jet or a submerged jet. Authors (Rao et al., 1971; Martin, 1977) have classified the flow regions on the target surface as the impingement region, the transition region, and the wall jet region. The impinging flow from multi-jets shows the same flow regions as a single jet, but in addition there are secondary stagnation zones where the wall jet of the adjacent nozzles impinge upon each other (Gardon and Cobonpue, 1962; Gardon and Akfirat, 1965; Korger and Krizek, 1966; Koopman and Sparrow, 1976). Multi-jets may exhibit 2 types of interactions (Koopman and Sparrow, 1976): (i) Possible interference between adjacent jets prior to their impingement on the surface, which depends on the spacing between jets and hence, the spacing between nozzle holes and their network arrangement; (ii) The second interaction is the collision of the surface flows (i.e. the wall jets) associated with adjacent impinging jets. The developing bell shape of the flow from the nozzle holes interferes with neighboring similar jet flows and results in local turbulence at the reacting surface. Thus, the flow patterns become more complex and are not so amenable to mathematical analysis. The flow patterns in single- and multi-jets are similar, but they may exhibit different levels of turbulence. In consideration of the complexity of mixed flow-patterns, an attempt has been made to interpret the flow behavior through empirical modeling.

Experimental Set-up and Procedure

A schematic diagram of the equipment and apparatus used in the present study is shown in Figure 1. The setup mainly consists of a storage tank (T), a pump (P), a rotameter (R), an electrolytic cell (C), and a manometer (M). The storage tank is made of copper sheet with a capacity of about 150 l and has a drain valve (V_1) at the bottom. The outlet line at the bottom of the tank is connected to the suction side of the pump and in between a valve (V_2) was provided to isolate the pump from the storage tank whenever necessary. A perforated coil (L) was placed inside the storage tank for deaeration. A 1.0 hp motor was used to drive the pump, which circulated the electrolyte solution. The outlet from the pump was divided into 2 lines: one for direct entry of the electrolyte solution into the cell through a rotameter and the other to serve as a by-pass, which returned to the storage tank (the by-pass being controlled by valve (V_3)). A rotameter made by Fischer and Porter, with a metering range of 0-20 l/min, was used to measure the electrolyte flow rate and was controlled by the valve (V_4) positioned at the upstream side of the rotameter.

Three different diameter electrolytic cells (C) (0.15 m, 0.20 m, and 0.25 m), each with identical cell height, were fabricated with rigid PVC tubes. The cells were rigidly fixed between 2 Hylam plates of the same dimensions using tie rods. The top Hylam plate of each cell was provided with 2 pipes; one served as the entry and the other served as an exit for the electrolyte solution. The bottom Hylam plate

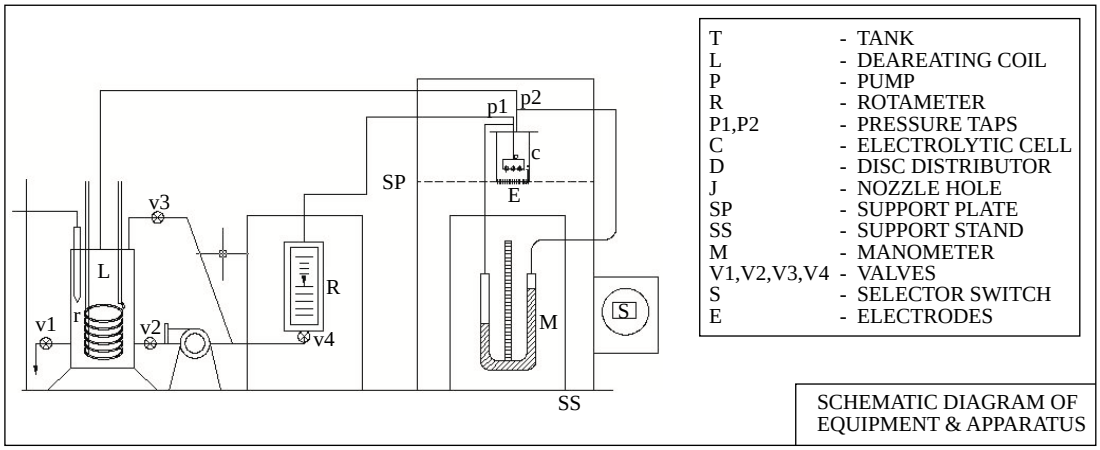

Figure 1. The schematic diagram of equipment and apparatus.

served as the target surface over which the ring electrodes were fixed flush with the surface, concentrically. A small disc electrode (E_1) 0.02 m in diameter cut out of a copper sheet was fixed at the center point of the target plate where the jet directly impinges. The geometrical distances of the ring electrodes were measured with respect to the center electrode (E_1). Each cell was also fitted with a copper strip 0.01 m wide fixed vertically flush to the inner wall of the cell, which served as the test electrode to obtain limiting current measurements at the wall. All the electrodes on the target plate and the wall electrode had copper terminals protruding outside for making the electrical connections. The inlet copper tube served as a counter electrode. The inlet and outlet copper tubes were provided with pressure taps (P1 and P2) for pressure drop measurements. A mercury manometer (M) was used to obtain the pressure drop data.

The nozzle hole assembly consisted of a disc distributor cut out of brass and the nozzles were drilled through the bottom section of the disc distributor, while the top section was connected to the inlet pipe running down through the top Hylam plate of the electrolytic cell. The height of the disc distributor from the target surface could be varied as desired with the help of a gland-and-nut system. A pointer scale (PS) was installed to note the height of the nozzle hole assembly from the target surface. The test cell, along with the nozzle hole assembly, was rigidly fixed to the supporting frame (SP) with appropriate level adjustment using a nut-and-screw arrangement and a spirit level. Copper wires soldered to the electrode terminals projecting outside were connected to a selector switch (S) to independently obtain the limiting current measurement at any desired electrode.

Limiting currents were measured for reduction of ferricyanide ion once the flow rate and temperature had stabilized. The electrochemical procedure adopted for the measurement was the same as described in an earlier study (Lin et al., 1951). An electric potential was applied in steps across the test and counter electrode and the corresponding currents were noted. The attainment of limiting current was observed by a sharp rise in potential for a small increase in current. The electrolyte consisted of equimolal solutions (0.01 M) of potassium ferricyanide and potassium ferrocyanide, with an excess indifferent electrolyte of 0.5 N sodium hydroxide. Measurements of limiting currents were obtained at different flow rates. The diameters of the electrolytic cells, disc distributors, nozzle holes, and height of the disc distributor varied and experiments were repeated for each case. For each individual run, the temperature remained constant within $\pm$ 0.1 °C, and if the temperature varied more than $\pm$ 0.1 °C the run was repeated. The electrolyte was analyzed for each and every run and the reproducibility of data was tested from time to time by repeating one of the previous runs under identical conditions. The ranges of variables covered are given in Table 1.

Results and Discussion

The existence and boundaries of various regions visualized on the target plate were identified and the data analyzed in terms of the regions and their combination as a single region based on the plots drawn for mass transfer coefficients (k_L) [calculated from limiting current density, similar to earlier studies (Rao et al., 1971; Venkateswarlu and Raju, 1979; Nanzer et al., 1984; Nanzer and Coeuret, 1984; Bensmaili and Coeuret, 1990a, 1990b; Bensmaili and Coeuret, 1995)] against the dimensionless average radial distance, 'x/D_c', for all the pertinent dynamic and geometric parameters covered in the present study.

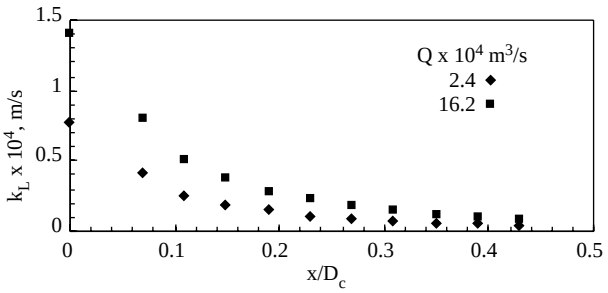

Figure 2. Variation of mass transfer coefficients with x/D_c from the center for different flow rates.

A close inspection of the trends in the plots, as represented in Figure 2, shows the existence of the following regions due to different flow patterns: (1) Impingement region wherein the limiting current densities are comparatively very high, which can also be referred to as the stagnation zone; (2) Transition region wherein the limiting current densities decrease with radial distance of the electrode; (3) Wall jet region wherein the limiting current densities decrease very slowly as compared to those in the transition region. The change from region 2 to region 3 is not abrupt, but smooth; hence, these 2 regions are

Table 1. Ranges of variables covered in the present study.

S. No:	Variable	Minimum	Maximum
1.	Flow rate ($Qx10^5$), m^3/s	4.0	27.0
2.	Velocity (v_{ef}), m/s	0.231	8.037
3.	Height of the nozzle assembly from the target surface, ($hx10^2$), m	1.0	25
4.	Diameter of the nozzle, ($dj\ x10^2$), m	0.1	0.2
5.	Diameter of disc distributor, ($D_d x10^2$), m	5.0	8.0
6.	Diameter of the cell, ($D_c x10^2$), m	15	25
7.	Average radial distance of the electrode on the target surface from the center, ($x * 10^2$), m	1.75	10.75
8.	Reynolds number, Re_{ef}	3757	70784
9.	Schmidt number, Sc	658	1063
10.	Froude number, Fr	0.368	1007.17

therefore combined to form a decreasing coefficient region. Prasad (1994) identified the existence of a similar decreasing coefficient region for the case of a submerged single jet. This current paper deals essentially with mass transfer in the impingement region, i.e. the stagnation point. The analysis of data in the decreasing coefficient region will be discussed in another paper as Part-II.

The mass transfer coefficient data plotted in Figure 2 show clearly that only the central electrode (E_1, at $x = 0$ or $x/D_c = 0$) covers the impingement region as the data of E_1 gave the highest values for the mass transfer coefficient, irrespective of the dynamic and geometric variables covered in the present study. Similar observations were reported even in the case of open free jets and submerged single jets (Chin and Tsang, 1978; Prasad, 1994; Bensmaili and Coeuret, 1995). The nozzle hole assembly used in the present case consists of a disc distributor containing nozzle holes of the same size (d_j) arranged in a triangular pitch network. Three different sizes of disc distributors (0.08, 0.06, and 0.05 m) with 55, 31, and 19 nozzle holes, respectively, are used in the present study. All the jets issuing through all the nozzle holes equally contribute to the generation of turbulence and the quantitative assessment of the impact appears to be complex. In view of this, the combined effect of all the nozzle holes is taken into consideration while computing the variable flow velocity, which defines the dynamic characteristic of the impinging jets.

In the case of multi-jets, it may be appropriate to define an equivalent nozzle diameter as that reported by Seung-Tae Koh et al. (1991) for a combination of jet nozzles. In the case of 'N' jet nozzles of the same size (d_j), the equivalent nozzle diameter, or effective diameter (d_{jef}), can be expressed as $\sqrt{N}xd_j$. The equivalent jet velocity, which is known as effective velocity (v_{ef}), based on the equivalent nozzle diameter, can be computed from the flow rate as follows:

$$v_{ef} = \frac{(4 \times Q)}{\left(\pi \times d_{jef}^2\right)} \tag{1}$$

This velocity is now taken as the mean velocity of the fluid-jet penetrating through the liquid column towards the target surface, which is calculated from the total mass flow rate.

Effect of Disc Distributor Height (h) from the Target Surface

The variation in the mass transfer coefficients with mean velocity, which is defined by Eq. (1) for a given D_c= 0.25 m, D_d= 0.08 m, and dj = 0.0015 m, and the heights of the jets (h) varying from 0.01 to 0.25 m for the central electrode on the target surface, are shown in Figure 3. An increased velocity increases the turbulence, which results in an increase in the coefficient up to 2-fold in the range of flow rates covered

in the present study. The increase in the coefficient is found to be gradual up to a certain velocity, and beyond this the increase in the coefficient is rapid. This sudden change in the trend is, however, found to be dependent on geometric variables, such as D_c, D_d, and d_{jef}, which are revealed in subsequent analysis of mass transfer data. The data of the plots in Figure 3 indicate that there exists a critical value for the flow (Q *or* v_{ef}) at which the change in the behavior of the coefficient is very conspicuous.

The plots also show a steady decrease in the mass transfer coefficient as the height of the disc distributor increases. As the height increases, the liquid jets that emerge from the nozzle holes may lose the impact of their momentum due to local flow interactions and collisions of adjacent jets. Thus, the impact of the jets may not fully reach the target surface where the mass transfer occurs. Similar observations were reported in earlier studies on single, open, free, and submerged jets (Chin and Tsang, 1978; Prasad, 1994; Bensmaili and Coeuret, 1995).

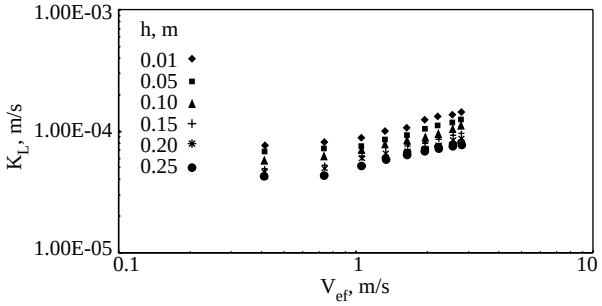

Figure 3. Variation of mass transfer coefficients with effective velocity for the central electrode (E_1) at different heights of the disc distributor.

Effect of the Diameter of the Disc Distributor (D_d)

In addition to being the potential sources for the jet-flow, the discs containing nozzle holes also serve as an efficient fluid distributor. The relative size of the disc containing these nozzle holes through which jet flow emerges affects the area swept by the issuing jets on the target surface, depending on the position of D_d from the target surface, i.e. h. Three different diameters of disc distributors have been used. The effect of D_d on the coefficients is shown in Figure 4. An increase in D_d, for a given flow rate or velocity, increases the area swept by impinging jets and a larger mass of fluid reaches the reacting surface, resulting in increased mass transfer.

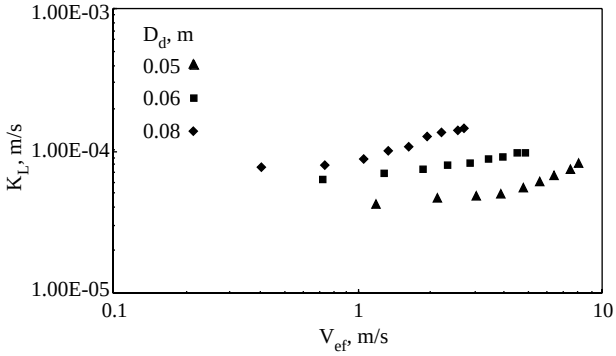

Figure 4. Variation of mass transfer coefficients with effective velocity for the central electrode (E_1) with different diameters of the disc distributor.

Effect of Nozzle Hole Diameter (d_j)

The dynamics of the emerging liquid jets are dependent on the size of the nozzle holes and the type of network in which they are arranged over the disc distributor, i.e. whether they are set in a triangular array or a square array. In the present case, however, studies have been carried out with only a triangular array. The plots of the data on mass transfer coefficients in Figure 5 demonstrate the effect of nozzle hole size on mass transfer coefficients. The plots of the data revealed that the coefficients increased with an increase in the nozzle hole size, which might be due to large-scale eddy turbulence at a given velocity.

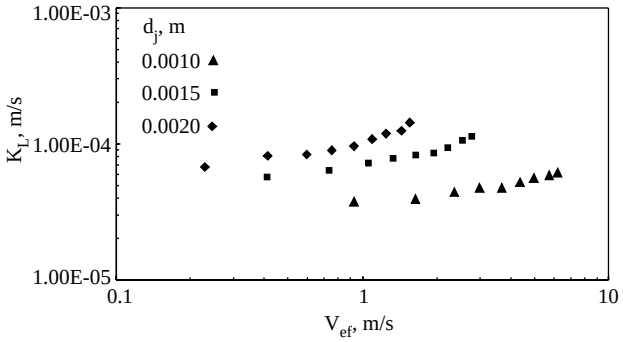

Figure 5. Variation of mass transfer coefficients with effective velocity for the central electrode (E_1) for different nozzle hole diameters.

Effect of Cell Diameter (D_c)

Three different sizes of cells (D_c) are used to investigate the effect of D_c on the transfer process at ring electrodes. For an increase in D_c, for a given flow

rate, the bulk average velocity (based on the cell size) falls, reducing the intensity of turbulence, which arises due to the free circulating flow patterns within the cell. Figure 6 demonstrates the effect of D_c on the transfer coefficients at a given flow rate, keeping the other geometric variables, d_{jef}, D_d, and h constant. A fall in the coefficient may be attributed to the reduced mass velocity associated with an increase in the cell diameter. A similar observation was even reported with single submerged jets (Prasad, 1994).

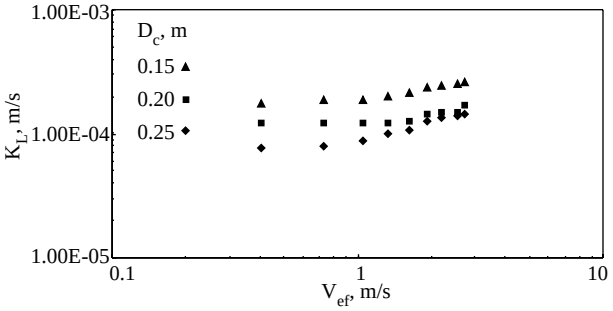

Figure 6. Variation of mass transfer coefficients with effective velocity for the central electrode (E_1) for different cell diameters.

Comparison with earlier studies

Figure 7 provides the present submerged multi-jet data in the impingement region [2], which are lower than the data of unsubmerged multi-jets reported by Bensmaili and Coeuret (1990b) [1]. However, the data of the present study showed coefficients higher than those of the submerged multi-jets of Bensmaili and Coeuret (1990a) [4] and Nanzer and Coeuret (1984) [5]. The heat transfer data of turbulent submerged liquid jets published by Chang et al. (1995) [3] are also shown in the same figure for comparison.

Figure 8 gives the comparison of the coefficients obtained from the study on free jets and single submerged jets in open containers with those obtained from the present data on multi-jets in the impingement region. The coefficient data of the present study [1], however, are much higher than those obtained with single submerged jets noted by Rao et al. (1971)[2] in open cells and the free multi-jets data of Venkateswarlu and Raju (1979) [3].

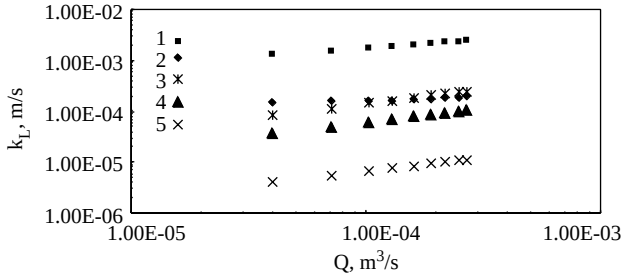

Figure 7. Comparison plots of the present study [2] with Bensmaili and Coeuret (free multi-jets) [1], Chang (submerged multi-jets [heat transfer]) [3], Bensmaili and Coeuret (submerged multi-jets) [4], and Nanzer and Coeuret (submerged multi-jets) [5].

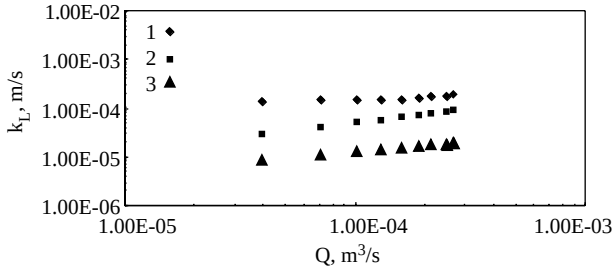

Figure 8. Comparison plots of the present study [1] with Rao et al. (single submerged jets in open container) [2] and Venkateswarlu and Raju (free multi-jets in open container) [3].

Correlations Developed

The issuing jet essentially influences the flow over the transfer surface and this depends on the effective nozzle hole diameter, d_{jef}, through which the jet is issuing. The size of the confining cell determines mass flow rates within the cell. The entire data showed 2 distinctly different regions: one for $d_{jef}/D_c \leq 0.037$ and the other for $d_{jef}/D_c > 0.037$. The analysis of the data carried out separately in the regions $d_{jef}/D_c \leq 0.037$ and $d_{jef}/D_c > 0.037$ revealed the existence of 2 different regimes, defined by the flow Reynolds number, based on the d_{jef} and v_{ef}, which exhibited in the plots of the data in Figure 9 for $d_{jef}/D_c > 0.037$ and Figure 10 for $d_{jef}/D_c \leq 0.037$. In the case of $d_{jef}/D_c > 0.037$, the data are divided into 2 regions, one for $Re_{ef} \leq 18{,}000$ and other for $Re_{ef} > 18,000$, while the data on $d_{jef}/D_c \leq 0.037$ showed a change in the trend at a critical Reynolds number of 30,000.

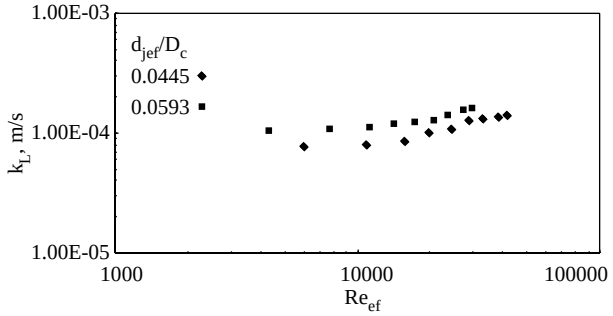

Figure 9. Variation of mass transfer coefficients with Reynolds numbers for $d_{jef}/D_c > 0.037$.

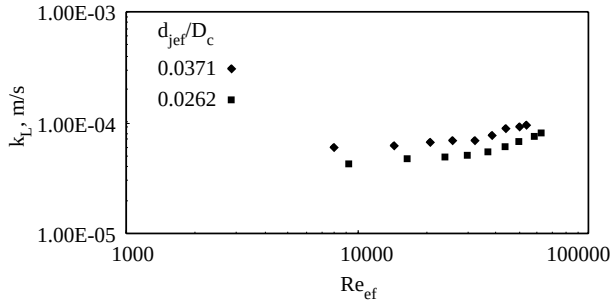

Figure 10. Variation of mass transfer coefficients with Reynolds numbers for $d_{jef}/D_c \leq 0.037$.

The compound effect of all the above could be expressed in terms of dimensionless geometric groups, which are subsequently used in the development of generalized correlations in the impingement region. The hydrodynamic conditions prevailing in the cell due to the interacting liquid jets through the circulating liquid flow are expected to generate thorough mixing of the fluid, thus promoting diffusion of the reacting species from the bulk to the electrode surface. The re-circulating flow, together with the multi-jet flow through the circulating liquid column, is assumed to generate secondary flows involving the gravitational/buoyancy and the centrifugal forces. The type of mixing that one can expect in the present case may be similar to that observed in an agitated vessel, and therefore these forces cause significant enhancement in the coefficients. The combined effect of the gravitational and centrifugal components of the forces due to secondary flows could be expressed in terms of the dimensionless Froude number, and incorporating this along with the Reynolds number and the pertinent geometric groups. The following format of equation has been used to develop generalized correlations by the regression analysis:

$$J_D = C(Re_{ef})_1^n (Fr)_2^n (\phi_1)_3^n (\phi_2)_4^n \qquad (2)$$

The data on reduction of ferricyanide ion in the impingement region yielded the following equations of correlation:

1. For $\mathbf{d_{jef}/D_c > 0.037}$

In the range of $Re_{ef} \leq 18{,}000$,

$$J_D = 6602.7(Re_{ef})^{-0.79}(h/D_d)^{-0.13}(d_{jef}/D_c)^{2.05}(Fr)^{-0.04}. \qquad (3)$$

In the range of $Re_{ef} > 18,000$,

$$J_D = 4.99(Re_{ef})^{-0.16}(h/D_d)^{-0.13}(d_{jef}/D_c)^{1.51}(Fr)^{-0.25}. \qquad (4)$$

2. For $\mathbf{d_{jef}/D_c \leq 0.037}$

In the range of $Re_{ef} \leq 30{,}000$,

$$J_D = 18.56(Re_{ef})^{-0.36}(h/D_d)^{-0.11}(d_{jef}/D_c)^{1.29}(Fr)^{-0.26}. \qquad (5)$$

In the range of $Re_{ef} > 30,000$,

$$J_D = 2.09(Re_{ef})^{-0.16}(h/D_d)^{-0.11}(d_{jef}/D_c)^{1.3}(Fr)^{-0.21}. \qquad (6)$$

The above equations are valid for the ranges of variables covered in the present study. The plots of the data correlated in accordance with Eqs. (3)-(6) (Correlation factor versus flow Reynolds number) are shown in Figures 11-14.

$$\text{Correlation factor } (cf) = J_D/((Fr)_2^n(\phi_1)_3^n(\phi_2)_4^n) \qquad (7)$$

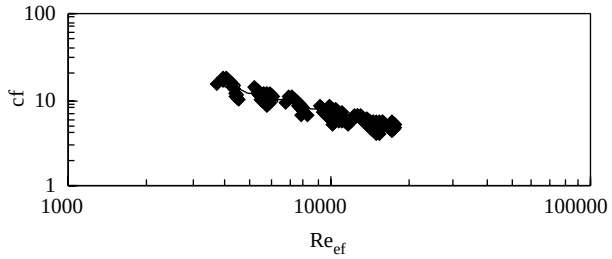

Figure 11. Correlation plot of Eq. (3) for $d_{jef}/D_c > 0.037$ and $Re_{ef} \leq 18,000$.

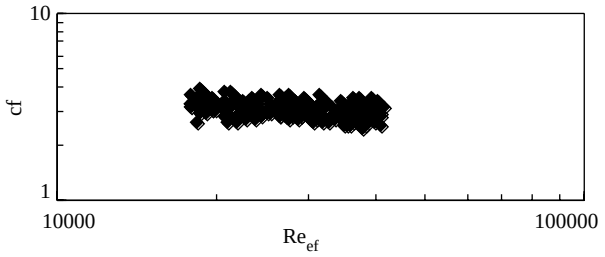

Figure 12. Correlation plot of Eq. (4) for $d_{jef}/D_c > 0.037$ and $Re_{ef} > 18,000$.

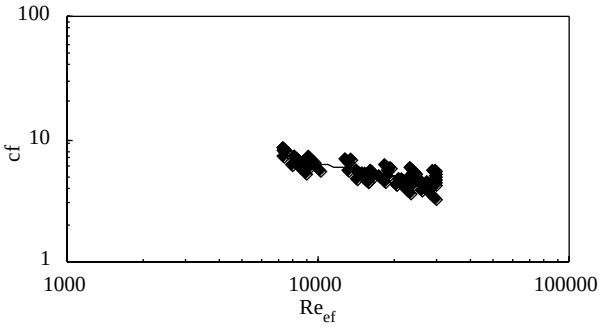

Figure 13. Correlation plot of Eq. (5) for $d_{jef}/D_c \leq 0.037$ and $Re_{ef} \leq 30,000$.

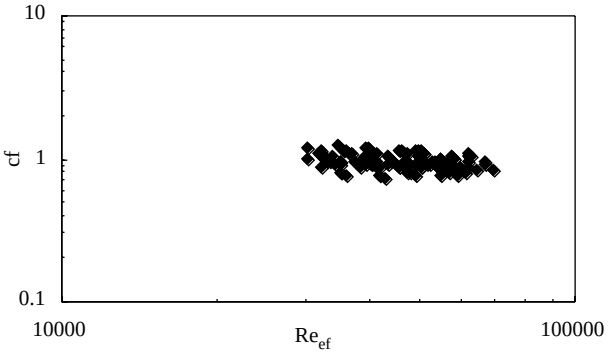

Figure 14. Correlation plot of Eq. (6) for $d_{jef}/D_c \leq 0.037$ and $Re_{ef} > 30,000$.

Conclusions

Multi-jet flow dynamics appears to be complex and the dynamic flow variable (v) has been computed taking into account all the jets issuing through all the nozzle holes. The discussion on the effects of the individual geometric parameters, such as d_{jef}, h, D_d, and D_c, on the transfer process in the impingement region lead to the following conclusions:

The coefficients decreased with an increase in the height of the distributor from target surface 'h', as the impact of jets may not have fully reached the target surface due to local flow interactions and collisions of adjacent jets.

The coefficients decreased with an increase in cell diameter D_c, and the bulk average velocity (based on cell diameter) fell, reducing the intensity of turbulence.

Increases in d_{jef} and D_d showed an increasing trend in the coefficients due to large scale eddy turbulence at a given velocity.

Two different flow regimes based on the ratio of d_{jef}/D_c and also on the Reynolds number have been identified and empirical correlations are proposed.

Acknowledgments

The authors are grateful to Professor C. Bhaskarasarma and Professor P. V. Ravi Kumar for their helpful discussions concerning this research.

Nomenclature

cf	correlation factor
C	constant
D_c	diameter of the cell, m
D_d	diameter of the disc distributor, m
D_L	diffusivity, m^2/s
d_j	diameter of the nozzle hole, m
d_{jef}	equivalent diameter $= \sqrt{N} \times d_j$, m
E_1	central electrode at $x = 0$ *or* $x/D_c = 0$
Fr	Froude number (v_{ef}^2/g d_{jef}).
g	acceleration due to gravity, m/s^2
h	height of the nozzle hole assembly from the target surface, m
J_D	mass transfer factor
k_L	mass transfer coefficient, m/s
N	number of nozzle holes on the disc distributor
Q	flow rate, m^3/s
Re_{ef}	Reynolds number based on d_{jef}, ($v_{ef} d_{jef} \rho/\mu$)
Sc	Schmidt number (μ/ρ D_L)
v_{ef}	velocity based on d_{jef}, m/s
x	average radial distance of the ring electrode on the target surface from the center of the cell, m
μ	viscosity of the electrolyte solution, kg/m
ρ	density of electrolyte solution, kg/m^3
ϕ	geometric parameters

References

Bensmaili, A. and Coeuret, F., "Transfert de Matiere Entre Une Nappe de Mercure et Des Jets Liquids Immerges, Simples Ou Multiples", The Can. J. Chem. Eng, [H.W. Wilson-AST]; 73, 85-94, 1995.

Bensmaili, A. and Coeuret, F., "Local Mass Transfer Coefficients at Wall Impinged by Submerged Multijets Issued from Very Porous Distributors", J. Electrochemical. Soc., 137, 1744-1750, 1990a.

Bensmaili, A. and Coeuret, F., "Overall Mass Transfer Between a Solid Surface and Submerged or Unsubmerged Liquid Multijets", J. Electrochemical. Soc., 137, 3086-3093, 1990b.

Chattopadhyay, H. and Saha, S.K., "Simulation of Laminar Slot Jets Impinging on a Moving Surface", Journal of Heat Transfer, 124, 1049-1055, 2002.

Chin, D.T. and Tsang, C.H., "Mass Transfer to an Impinging Jet Electrode", Journal of Electrochemical Society, 125, 1461-1469, 1978.

Chang, C.T., Kojasoy, G. and Landis, F., "Confined Single- and Multiple-jet Impingement Heat Transfer-I. Turbulent Submerged Liquid Jets", International Journal of Heat and Mass Transfer, 38, 833-842, 1995.

Gardon, R. and Cobonpue, J., "International Developments in Heat Transfer", ASME, New York, 454, 1962.

Gardon, R. and Akfirat, J.C., "The Role of Turbulence in Determining the Heat Transfer Characteristics of Impinging Jets", Int. J. Heat and Mass Transfer, 8, 1261-1272, 1965.

Korger, M. and Krizek, F., "Mass Transfer Coefficient in Impingement Flow from Slotted Nozzles", Int. J. Heat and Mass Transfer, 9, 337-344, 1966.

Koopman, R.N. and Sparrow, E.M., "Local and Average Transfer Coefficients Due to an Impinging Row of Jets", Int. J. Heat and Mass Transfer, 19, 673-683, 1976.

Lin, C.S., Denton, E.B., Gaskill, H.S. and Putnam, G.L., "Diffusion Controlled Electrode Reactions", Industrial and Engineering Chemistry, 43, 2136-2143, 1951.

Martin, H., "Heat and Mass Transfer Between Impinging Gas Jets and Solid Surfaces", Advances in Heat Transfer, 13, 1-60, 1977.

Nanzer, J., Donizeau, A. and Coeuret, F., "Overall Mass Transfer between Electrodes and Normal Impinging Submerged Multijets of Electrolyte", J. Applied Electrochemistry, 14, 51-62, 1984.

Nanzer, J. and Coeuret, F., "Distribution of Local Mass Transfer Coefficients over One Electrode Bombarded by Submerged Multijets of Electrolyte", J. Applied Electrochemistry, 14, 627-638, 1984.

Prasad, V.S.R.K., "Studies on Ionic Mass Transfer with Impinging Submerged Jets in Closed Cylindrical Cells", PhD Thesis, Andhra University, Visakhapatnam, 1994.

Subba Rao, B., Krishna, M.S. and Raju, J.G.J.V., "Ionic Mass Transfer with Submerged Jets-I", Per. Pol. Ch 17, 185-195, 1971.

Tae Koh, S., Hiraoka, S., Tada, Y., Takahashi, T. and Yamaguchi, T., "Heat Transfer Coefficient and Mixing Time in a Cylindrical Mixing Vessel with Axial Jet Nozzles", Journal of Chemical Engineering of Japan, 24, 506-510, 1991.

Venkateswarlu, P. and Jagannadha Raju, G.J.V., "Ionic Mass Transfer with Impinging Multi-jets", Indian J. Technol., 17, 1-4, 1979.